Nuclear level densities of ^{64,66}Zn from neutron evaporation

A. P. D. Ramirez,* A. V. Voinov, S. M. Grimes, A. Schiller, C. R. Brune, and T. N. Massey
Ohio University, Athens, Ohio 45701, USA

A. Salas-Bacci
University of Virginia, Charlottesville, Virgina 22904, USA

(Received 25 September 2013; published 26 December 2013)

Double differential cross sections of neutrons from $d + {}^{63,65}$Cu reactions have been measured at deuteron energies of 6 and 7.5 MeV. The cross sections measured at backward angles have been compared to theoretical calculations in the framework of the statistical Hauser-Feshbach model. Three different level density models were tested: the Fermi-gas model, the Gilbert-Cameron model, and the microscopic approach through the Hartree-Fock-Bogoliubov method (HFBM). The calculations using the Gilbert-Cameron model are in best agreement with our experimental data. Level densities of the residual nuclei ^{64}Zn and ^{66}Zn have been obtained from statistical neutron evaporation spectra. The angle-integrated cross sections have been analyzed with the exciton model of nuclear reaction.

DOI: 10.1103/PhysRevC.88.064324 PACS number(s): 21.10.Ma, 24.60.Dr, 25.45.−z, 27.50.+e

I. INTRODUCTION

Nuclear reaction codes are commonly used in basic and applied nuclear science, particularly in calculating reaction cross sections. A primary example is in the area of astrophysics where cross sections from a wide variety of nuclear processes play a crucial role as one of the inputs in modeling stellar evolution and nucleosynthesis. The predictive power of these codes has proven helpful especially in regimes where accelerator-based experiments fail to imitate the environment of astrophysical processes. However, the reliability of nuclear reaction codes to provide accurate cross sections depends on the accuracy of their input parameters.

The statistical Hauser-Feshbach (HF) theory [1] is the main tool to calculate cross sections for nuclear reactions at low incident energies. In these reactions, the compound mechanism is responsible for at least 90% of the total reaction cross section. The HF model requires the knowledge of transmission coefficients and nuclear level densities. Particle transmission coefficients are derived using the Schrödinger equation from generally known optical model potentials (OMP) of the particle-nucleus interaction. Transmission coefficients of γ rays, however, are calculated from γ strength functions. Both OMP and γ strength functions assume typical functional forms and these are optimized from the elastic scattering data and the analysis of the photoabsorption cross sections. Similarly, level densities are determined through phenomenological analytical expressions or microscopic calculations.

Most of the effort in improving the HF calculations goes to the nuclear level density (NLD), which is known to cause the largest uncertainty in the calculated cross sections. Typical phenomenological NLD models employ the basic Fermi gas level density form [2] given by

$$\rho(U) = \frac{1}{12\sqrt{2}}\frac{1}{\sigma a^{1/4}}\frac{\exp\left[2\sqrt{a(U-\delta)}\right]}{(U-\delta)^{5/4}}, \qquad (1)$$

where a is the level density parameter, δ is the pairing and shell shift, σ is the spin cut-off parameter, and U is the excitation energy. Slight modifications of this expression are usually done to account for important correlations such as shell effects, pairing, collective enhancements and isospin dependence, and to produce agreement with existing experimental data.

Several systematics for phenomenological NLD models are well documented in the literature for a wide range of mass numbers [3,4]. In these systematics, parameters were obtained by fitting the density of discrete levels using the experimental level scheme in the low excitation energies and the neutron resonance spacing near the neutron binding energy. Because of the lack of experimental information between these regions, model interpolations might be uncertain. Also, the spin cutoff parameter is not well known near the neutron binding energy. Calculating level densities for spins other than spins of neutron resonances is problematic. Developing other experimental methods based not only on neutron resonance data is necessary to constrain and improve level density parametrizations.

The microscopic description of the level density has also made some progress in the last decades [5–7]. It was found to agree well with some of the highly parametrized phenomenological models in describing experimental data. Logically, the microscopic approach should provide a better description especially in regions where no experimental information is available, such as at very high excitation energies or for nuclei far from the valley of stability, although this remains to be confirmed.

In this paper we study the level densities of ^{64,66}Zn up to the neutron binding energy by analyzing evaporated neutrons from $d + {}^{63,65}$Cu reactions. This method was confirmed to be reliable in the case of compound reactions [8]. Although, deuteron-induced reactions cannot be considered as purely compound, neutron spectra measured at backward angles with 7-MeV deuterons are shown to contain negligible noncompound components [9]. Moreover, the evaporation method is less sensitive to spin and parity distributions, which makes it advantageous compared to the method based on neutron resonance counting.

*ar765608@ohio.edu

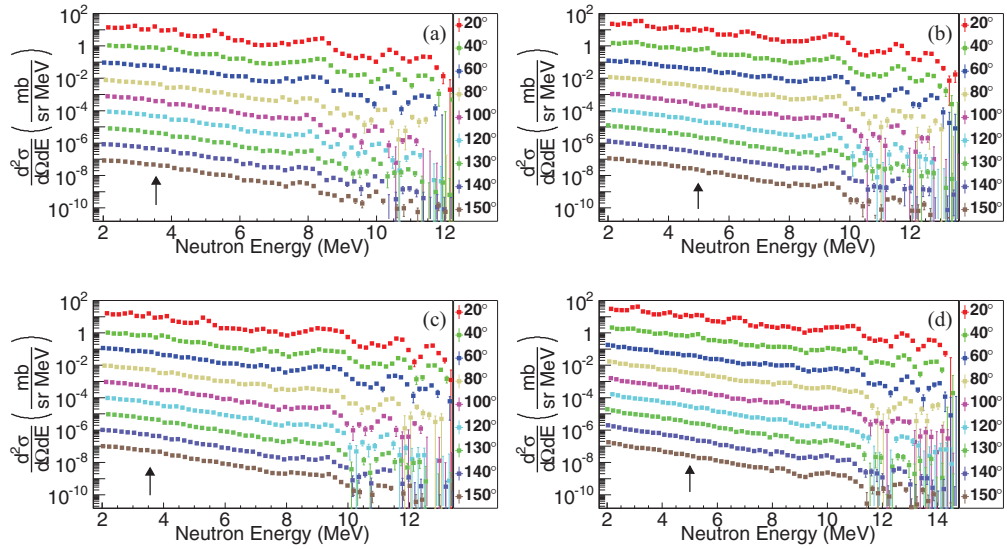

FIG. 1. (Color online) Double differential cross sections in the center-of-mass frame of ^{63}Cu(d,n) for deuteron energies of (a) 6 and (b) 7.5 MeV and ^{65}Cu(d, n) for (c) 6 and (d) 7.5 MeV. The error bars represent statistical errors only. The cross section from each angle is scaled down by a factor of 0.1 as the angle is increased.

II. EXPERIMENT

The experiment was performed at the Edwards accelerator laboratory of Ohio University using the 4.5-MV tandem Van de Graaff accelerator. The targets consisted of self-supporting 2-mg/cm^2 ^{63,65}Cu foils, which were isotopically enriched to 99.8% and 99.7%, respectively. The targets were bombarded by 6 and 7.5 MeV deuterons. Outgoing neutrons were registered using three NE213 neutron detectors, which were positioned inside an underground tunnel to reduce background radiation. Neutron energies were obtained by the time-of-flight (TOF) technique with a flight path of 6.93 m. The time calibration of the detectors was done by producing peaks in the TOF spectrum at regular intervals with a pulse generator. The nonlinear relationship of channel and time was taken into account by measuring the time uncorrelated distribution from a γ source. The γ peak in the spectrum was employed to make the absolute time calibration. We obtained the efficiency of the scintillation detectors with the standard neutron spectrum from the ^{27}Al(d,n) reaction at an energy of 7.44 MeV and angle of 120° [10]. This method allows the efficiency to be measured in the energy interval 2–14 MeV, the same energy interval in which we are interested. The efficiency was found to be ∼15% for the neutron energy of 2 MeV and it decreases to ∼8% for the neutron energy of 14 MeV. We acquired the beam intensity from the beam current collected by the Faraday cup. Since the detectors are sensitive to both γ rays and neutrons, pulse shape discrimination (PSD) was utilized to identify the neutrons. The neutron gated TOF spectrum was transformed to the neutron energy spectrum by using the time calibration and the neutron flight path. From the information about the target thickness, the integrated beam current and the detector efficiency, cross sections were calculated. The neutron emission spectra were measured at angles of 20°, 40°, 60°, 80°, 100°, 120°, 130°, 140°, and 150°. This was done with the swinger facility where the swinger beam leg along with the attached target chamber rotate at an axis where the scattering target is located while the detectors were set fixed in the tunnel.

III. DATA ANALYSIS AND RESULTS

To compare our results with the calculations, double differential cross sections were converted to the center-of-mass (c.m.) system. This was done by using two-body kinematics and assuming that the cross sections were due only to the ^{x}Cu(d,n)$^{x+1}$Zn reactions. The c.m. and laboratory scattering angles vary at most by a couple of degrees. Figure 1 shows the inclusive neutron spectra from all the reactions. Inclusive means that neutrons emitted from the later stages other than the primary stage of the (d,n) reaction are included in the spectra. The upper neutron energy limits where multiple stage contributions are energetically possible are marked by the arrows in the figure. Above this energy, only the first stage neutrons contribute to the spectra.

The angular distributions for selected energy intervals are shown in Fig. 2. Each point refers to the integrated cross sections over the given energy interval for a particular angle. The peaking of the distributions in the forward angles is attributed to direct and pre-equilibrium components of the reactions. The compound contribution, however, is known to be symmetric at 90° in the c.m. frame. Since the measured cross sections do not vary a lot at backward angles, we assumed that these were dominated by the compound reaction mechanism. This is also consistent with our estimation that the degree of anisotropy for deuteron-induced compound reactions at these energies and mass range should not exceed 10%. These data were averaged from 120° and above to improve the statistics and they were used to represent the compound component for the rest of the paper. The solid curve is a fit utilizing the phenomenological Kalbach formula [11] for the continuum

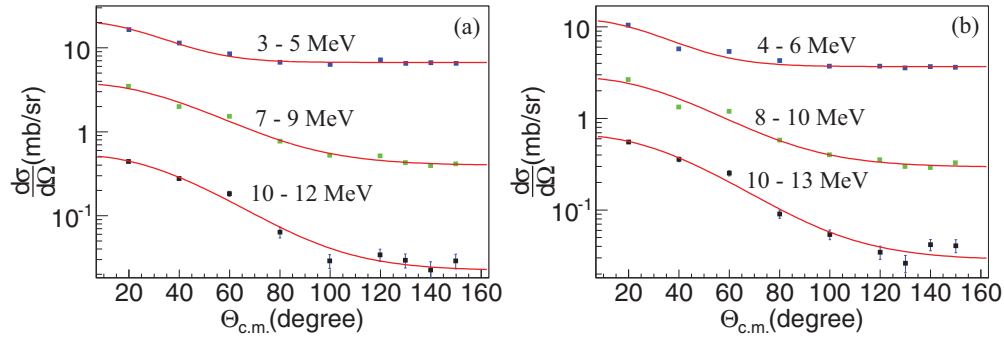

FIG. 2. (Color online) Angular distributions of (a) ^{63}Cu(d,n) and (b) ^{65}Cu(d,n) for incident deuteron energy of 6 MeV taken from selected neutron energy intervals. The solid line is a fit from the Kalbach formula given in Eq. (2).

angular distribution given by

$$\sigma(\theta) = C\{\exp(a_d \cos\theta) + R[\exp(a_c \cos\theta) + \exp(-a_c \cos\theta)]\}. \quad (2)$$

The first term describes the forward peaked component and the second one with the relative contribution R is related to the symmetric component of the angular distribution. Parameters a_d and a_c describe the steepness of the slope for both direct and compound components, respectively.

According to the authors of Ref. [11] the symmetric component may also include the contribution from multistep compound mechanism of the nuclear reaction. We assumed here that at our low deuteron energies the symmetric component of the angular distribution is due to the compound reaction mechanism only.

Equation (2) was used to quantitatively estimate the compound and noncompound components of the reaction cross sections. We found that for ^{63}Cu(d,n)^{64}Zn, the noncompound fractions at 6- and 7.5-MeV incident energies are 22% and 27%, respectively. For ^{65}Cu(d,n)^{66}Zn, these are 17% at 6 MeV and 25% at 7.5 MeV. The decrease of the compound fraction as the beam energy increases is expected, which is also observed in Ref. [12]. Therefore, for the level density study where compound reactions are utilized, we used the data obtained with the incident beam energy of 6 MeV. We also reduced the theoretical calculations by these fractions when compared to the experimental data.

Theoretical calculations were performed using the EMPIRE code [13]. Transmission coefficients were calculated from the default optical model parameters provided by the code, which uses the Reference Input Parameter Library (RIPL) [14]. Three different level density models were tested: the Fermi gas model (FGM) [Eq. (1)] implementing the global parameters of the Egidy systematics [3]; the Gilbert-Cameron model (GCM) [15] with parameter systematics from Ref. [14], which uses the constant temperature model in the low excitation energy region and the FGM at high excitation energies; and the microscopic combinatorial approach [7] where the single-particle level schemes were generated by the Hartree-Fock-Bogoliubov (HFBM) method. For the FGM with the Egidy parameter systematics, the parameter a is calculated in terms of the deuteron pairing energies and the shell corrections according to Ref. [3]. The spin cutoff parameter is calculated with the following expression [16]

$$\sigma^2 = 0.0146A^{5/3}\frac{1+\sqrt{1+4a(U-\delta)}}{2a}. \quad (3)$$

For the FGM, which is part of the GCM, the parameter a is determined according to Ref. [17] by the expression

$$a(U) = \tilde{a}\left\{1+[1-\exp(-\gamma U)]\frac{\delta W}{U}\right\}. \quad (4)$$

where $\tilde{a}$ is the asymptotic level density parameter, δW is the shell correction and γ is the shell damping parameter. The negative and positive parities are considered to be equal. The temperature T is adjusted for the constant temperature part such that the level density is consistent with the discrete level density at low energies and with the Fermi-gas model at high energies according to Ref. [13]. Also, the important point is that the level density parameter a in all parameter systematics which are based on the analysis of neutron resonance data is considered to be dependent on shell corrections.

The spin cutoff parameter for the GCM is based on the following formula

$$\sigma^2 = 0.146A^{2/3}\sqrt{a(U-\delta)} \quad (5)$$

for the Fermi-gas part of the GCM. The constant temperature part uses linear interpolation between the spin cutoff parameter of the discrete levels and the formula above at the matching energy.

The experimental differential cross sections that are due to the compound reaction mechanism were obtained by averaging the double differential cross sections measured at backward angles and by multiplying them by 4π. Figure 3 shows the neutron emission spectra for 6-MeV bombarding energy. These spectra are compared to the predictions from EMPIRE. The calculations using the microscopic HFBM show slight deviation particularly at high neutron energies. Both the FGM and the GCM reproduce the data well for the whole energy range even though tiny deviations at the highest and lowest neutron energies can be observed. For the GCM we tested two sets of parameters according to the Ignatyuk systematics [17] and the Iljinov systematics [4]. We found that the best agreement was achieved using Ref. [17] for ^{64}Zn and Ref. [4] for ^{66}Zn. Using the same, either Ref. [17] or Ref. [4] systematics for both nuclei gives us worse agreement with the

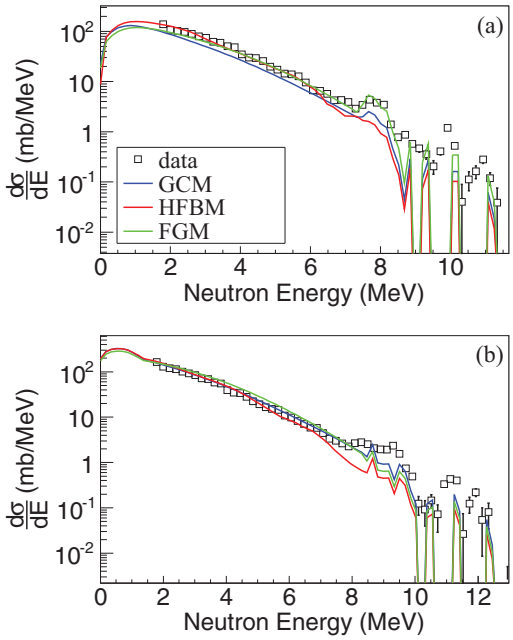

FIG. 3. (Color online) Experimental differential cross sections compared to theoretical calculations using different input level density models for (a) ^{63}Cu(d,n) and (b) ^{65}Cu(d,n) for the 6-MeV incident deuteron energy.

experimental data points for one of these nuclei. The same systematics predict 20% difference in temperature T and a for ^{64}Zn versus ^{66}Zn (see Table I), which is not supported by the experimental data. The data indicate that the temperatures for ^{64}Zn and ^{66}Zn nuclei are the same within 2%.

When the best parameters were used to calculate the differential cross sections for 7.5-MeV deuteron energy, the enhancement of the experimental points relative to calculations (see Fig. 4) was observed in the region of high neutron energies. Such enhancement is attributed to noncompound mechanisms that contribute to the cross sections. This observation is seen in both $d + ^{63,65}$Cu reactions.

TABLE I. Parameters used in the Gilbert-Cameron and Fermi gas level density models for the theoretical calculations. Best GCM parameters to reproduce the data are underlined.

	GCM Parameters					
Nucleus	$\tilde{a}$	U_x	δ	E_0	T	Ref.
^{64}Zn	10.11	8.08	3.0	−0.30	1.07	[17]
	8.86	9.49	3.0	−0.93	1.23	[4]
^{66}Zn	10.43	6.62	2.95	0.42	0.93	[17]
	9.12	7.92	2.95	−0.14	1.09	[4]

	FG Parameters	
Nucleus	a	δ
^{64}Zn	7.38	1.02
^{66}Zn	8.14	0.96

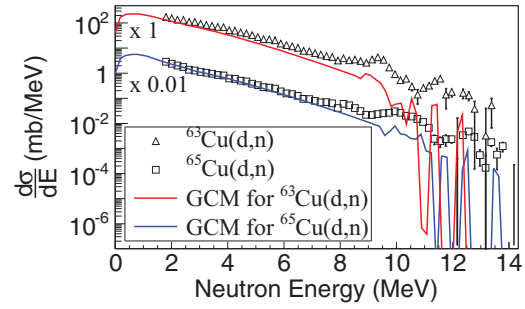

FIG. 4. (Color online) Differential cross sections obtained with the 7.5-MeV incident energy for ^{63}Cu(d,n) (top) and ^{65}Cu(d,n) (bottom) (a factor of 0.01 was used for distinction). The predictions were calculated based on the best GCM parameters found in Table I.

The experimental level densities $\rho(E)_{\rm exp}$ were extracted using the following expression [18]

$$\rho(E)_{\rm exp} = \rho(E)_{\rm model} \frac{(d\sigma/d\epsilon)_{\rm exp}}{(d\sigma/d\epsilon)_{\rm model}}, \qquad (6)$$

where $(d\sigma/d\epsilon)_{\rm exp}$ is the differential cross section from the experiment and $(d\sigma/d\epsilon)_{\rm model}$ is the differential cross section calculated by EMPIRE using $\rho(E)_{\rm model}$ as its input level density. The $\rho(E)_{\rm exp}$ cannot be obtained in absolute units from Eq. (6) alone because the ratio of $(d\sigma/d\epsilon)_{\rm exp}/(d\sigma/d\epsilon)_{\rm model}$ depends not only on the ratio $\rho(E)_{\rm exp}/\rho(E)_{\rm model}$, but also on the competition with other channels such as (d, p). In the present study we did not analyze the (d, p) channel, therefore the level density obtained with Eq. (6) has been independently normalized to the density of known levels in the discrete level region.

Figure 5 shows the level density $\rho(E)_{\rm exp}$ for ^{64,66}Zn. It should be mentioned that the error bars of the data points shown in the figure are due to statistics only. An additional 15% for the overall systematic uncertainty should be added in quadrature with the statistical error to obtain the total uncertainty. There is a good agreement between the level densities extracted

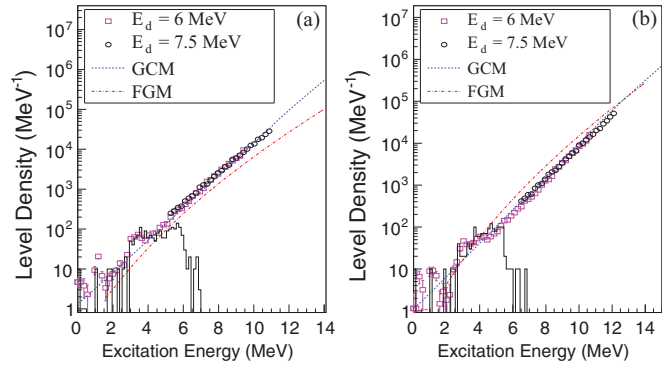

FIG. 5. (Color online) Level density versus the excitation energy for (a) ^{64}Zn and (b) ^{66}Zn. The data for 6-MeV incident energy (square) and 7.5 MeV (circle) were normalized to the discrete low lying levels (histogram). The experimental level densities were compared to the NLD models: FGM (dashed-dotted red line) with Egidy parameters systematics [3] and GCM (dashed blue line) with parameters systematics according to Ref. [17] and Ref. [4] for ^{64}Zn and ^{66}Zn, respectively.

from cross sections measured with 6- and 7.5-MeV deuteron energies. At the lower excitation energy region populated by high energy neutrons only the data points obtained from 6-MeV deuteron-induced reactions are presented. High energy neutrons produced by 7.5-MeV deuterons are partly due to the noncompound reaction mechanism (see Fig. 4). Therefore corresponding cross sections have not been used to deduce the level densities at low excitation energy region of ^{64,66}Zn nuclei.

Experimental level density values were fitted using the constant temperature model for both reactions and it was found that a slight change in slope is observed with bombarding energies. The temperatures of ^{64}Zn at deuteron energies of 6 and 7.5 MeV were determined to be 1.10(2) and 1.19(2) MeV, respectively, while that for ^{66}Zn were 1.08(2) and 1.18(2) MeV. The change in temperature may have resulted from the pre-equilibrium contribution for the data with higher bombarding incident energy. The pre-equilibrium mechanism enhances the higher energy portion of the neutron spectrum more than the lower energy part. We also observed a noticeable step structure from the extracted level densities starting at excitation energies ∼3 and ∼2.5 MeV for ^{64}Zn and ^{66}Zn, respectively. It has been proposed that such a structure might be related to the breaking of the nucleon Cooper pairs [19]. The broken pairs introduce new degrees of freedom leading to an increase of level density.

A comparison of the extracted level density to NLD models is presented in Fig. 5. Despite the good agreement between experimental and calculated cross sections using FGM (as shown in Fig. 3), the FGM level densities exhibit some offset relative to the experimental ones. Also the slope of the FGM function for ^{64}Zn is not consistent with the experimental data and it is different compared to ^{66}Zn. This observation is consistent with global systematics for GCM which also predict different slopes for ^{64}Zn versus ^{66}Zn. Experimental data points exhibit the same slope within 2%. The different slopes determined by parameters a and T in GCM and by parameter a in FGM are due to different values of the shell correction δW in Eq. (4). The same slope of experimental NLD for ^{64,66}Zn indicates the fact that the shell correction has negligible effect on level density parameters for both nuclei.

The angle-integrated cross sections shown in Fig. 6 were obtained by integrating the angular distribution fit using Eq. (2) over all solid angles. The cross sections were then compared to pre-equilibrium model calculations. As it is seen in the angular distributions (see Fig. 2), noncompound contributions to the cross sections are present in our data. We also included the calculated cross section which is due to the compound reaction. The calculations were made by EMPIRE [13] and TALYS [20] codes. In EMPIRE, we applied the PCROSS module that incorporates the one-component exciton model and also includes the Iwamoto-Harada model that considers the pre-equilibrium mechanism for clusters in the incoming and outgoing channels [13]. For TALYS, we chose to use the two-component exciton model [20], which treats proton and neutron excitons separately, over the one-component exciton model. The former is expected to better describe the data since it is an improvement of the latter. Also, calculations with both

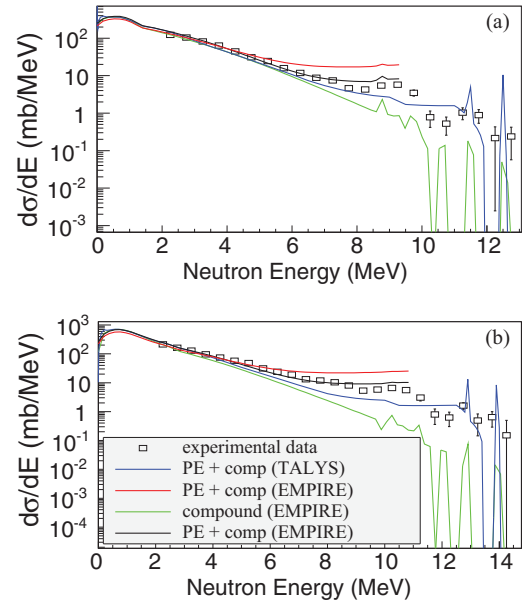

FIG. 6. (Color online) Experimental angle-integrated differential cross sections for ^{65}Cu(d,Xn) at energies (a) 6 and (b) 7.5 MeV. Solid lines are EMPIRE and TALYS calculations. PE and comp stand for pre-equilibrium and compound components, respectively. The red solid line has its mean free path set to 1.3, which is the default value while the black solid line has it set to 0.5.

models do not differ significantly. We used the level density parameters obtained by fitting our data for 6-MeV deuteron energy with the constant temperature model.

Exciton models generally improve the description of angle-integrated experimental cross sections. However, calculations show that neither EMPIRE nor TALYS allow us to reproduce the data points with the default parameters of exciton models. EMPIRE overestimates the angle-integrated cross sections while TALYS underestimates them. We adjusted the mean free path parameter of the PCROSS model to 0.5 from the default value of 1.3 for EMPIRE to reproduce the experimental results. It should be noted that the direct reaction mechanism is taken into account in the TALYS calculations and that it contributes primarily to the discrete states populated by the high energy neutrons.

IV. SUMMARY AND CONCLUSION

The double differential cross sections for $d + ^{63,65}$Cu reactions have been measured with 6- and 7.5-MeV deuteron beams. Cross sections from backward angles have been compared to HF calculations with the EMPIRE computer code using different input level density models. The Gilbert-Cameron model was found to describe the experimental data best. The temperature T that determines the slope of level density functions was found to be the same within 2% for ^{64}Zn and ^{66}Zn nuclei. This is in contradiction with commonly used systematics [4,17] that predict the difference in T of about 20%. The same is true for FG parameter systematics of Ref. [3] which gives different slopes of level density functions

that is not consistent with our experimental results. It is also important to note that the shape of experimental level density functions are in better agreement with the constant temperature part of the Gilbert-Cameron model rather than with the basic Fermi-gas model.

Angle-integrated cross sections were found to contain the component which increases the cross sections of high energy neutrons. Experimental cross sections for both ^{63,65}Cu(d,n) reactions have been compared to exciton model calculations with EMPIRE and TALYS computer codes. Using the exciton model improves the description of the angle integrated cross sections although parameters still need to be adjusted to reach more accurate agreement.

ACKNOWLEDGMENTS

This work was supported in part by the U.S. Department of Energy under Grants No. DE-FG02-88ER40387, DE-FG52-09NA29455, and DE-NA0001837. We also acknowledge D. K. Jacobs, J. E. O'Donnell, and D. E. Carter for the technical help during the experiments in the Edwards accelerator laboratory.

[1] L. Wolfenstein, Phys. Rev. **82**, 690 (1951); W. Hauser and H. Feshbach, *ibid*. **87**, 366 (1952).
[2] H. A. Bethe, Phys. Rev. **50**, 332 (1936).
[3] T. von Egidy and D. Bucurescu, Phys. Rev. C **72**, 044311 (2005).
[4] A. S. Iljinov and M. V. Mebel, Nucl. Phys. A **543**, 517 (1992).
[5] Y. Alhassid, S. Liu, and H. Nakada, Phys. Rev. Lett. **83**, 4265 (1999).
[6] S. Hilaire, J. P. Delaroche, and M. Girod, Eur. Phys. J. A **12**, 169 (2001).
[7] S. Goriely, S. Hilaire, and A. J. Koning, Phys. Rev. C **78**, 064307 (2008).
[8] R. Fischer, G. Traxler, M. Uhl, and H. Vonach, Phy. Rev. C **30**, 72 (1984).
[9] A. V. Voinov, S. M. Grimes, C. R. Brune, M. J. Hornish, T. N. Massey, and A. Salas, Phys. Rev. C **76**, 044602 (2007).
[10] T. N. Massey, S. Al-Quraishi, C. E. Brient, J. F. Guillemette, S. M. Grimes, D. K. Jacobs, J. E. O'Donnell, J. Oldendick, and R. Wheeler, Nucl. Sci. Eng. **129**, 175 (1998).
[11] C. Kalbach, Phys. Rev. C **37**, 2350 (1988).
[12] S. I. Al-Quraishi, C. E. Brient, S. M. Grimes, T. N. Massey, J. Oldendick, and R. Wheeler, Phys. Rev. C **62**, 044616 (2000).
[13] M. Herman, R. Capote, B. V. Carlson, P. Oblozinsky, M. Sin, A. Trkov, H. Wienke, and V. Zerkin, Nucl. Data Sheets **108**, 2655 (2007).
[14] R. Capote, M. Herman, P. Oblozinsky, P. G. Young, S. Goriely, T. Belgya, A. V. Ignatyuk, A. J. Koning, S. Hilaire, V. A. Plujko, M. Avrigeanu, O. Bersillon, M. B. Chadwick, T. Fukahori, Z. Ge, Y. Han, S. Kailas, J. Kopecky, V. M. Maslov, G. Reffo, M. Sin, E. Sh. Soukhovitskii, and P. Talou, Nucl. Data Sheets **110**, 12 (2009).
[15] A. Gilbert and A. G. W. Cameron, Can J. Phys. **43**, 1446 (1965).
[16] H. Zhongfu, H. Ping, S. Zongdi, and Z. Chunmei, Chin. J. Nucl. Phys. **13**, 147 (1991).
[17] A. V. Ignatyuk, G. N. Smirenkin, and A. S. Tishin, Sov. J. Nucl. Phys. **21**, 255 (1975).
[18] H. Vonach, Proceedings of the IAEA Advisory Group Meeting on Basic and Applied Problems of Nuclear Level Densities, Upton, NY, 1983, BNL Report No. BNL-NCS-51694, 1983, p. 247.
[19] E. Melby, L. Bergholt, M. Guttormsen, M. Hjorth-Jensen, F. Ingebretsen, S. Messelt, J. Rekstad, A. Schiller, S. Siem, and S. W. Odegard, Phys. Rev. Lett. **83**, 3150 (1999).
[20] A. J. Koning, S. Hilaire, and M. C. Duijvestijn, in TALYS-1.0, *Proceedings of the International Conference on Nuclear Data for Science and Technology, April 22–27, 2007, Nice, France*, edited by O. Bersillon, F. Gunsing, E. Bauge, R. Jacqmin, and S. Leray, (EDP Sciences, Les Ulis, France, 2008), pp. 211–214.